Reaching ultra-high vacuum for a large vacuum vessel in an underground environment

D. O. Sabulsky[1], *X.* Zou[1], *J.* Junca[1], *A.* Bertoldi[1], *M.* Prevedelli[2], *Q* Beaufils[3], *R* Geiger[3], *A.* Landragin[3], *D.* Boyer[4], *S.* Gaffet[4], *P* Bouyer[1], and *B.* Canuel[1,*]

[1]LP2N, Laboratoire Photonique, Numérique et Nanosciences, Université Bordeaux–IOGS–CNRS:UMR 5298, rue F. Mitterrand, F–33400 Talence, France
[2]Dipartimento di Fisica e Astronomia, Università di Bologna, Via Berti-Pichat 6/2, I-40126 Bologna, Italy
[3]LNE–SYRTE, Observatoire de Paris, Université PSL, CNRS, Sorbonne Université, 61, avenue de l'Observatoire, F–75014 Paris, France
[4]LSBB, Laboratoire Souterrain à Bas Bruit, CNRS UAR3538, Avignon University - La grande combe, 84400 Rustrel, France

Abstract. Located far from anthropical disturbances and with low seismic and magnetic background noise profiles, the LSBB facility is the ideal location for a new hybrid detector for the study of space-time strain. The MIGA infrastructure [1], utilizes an array of atom interferometers manipulated by the same beam, the resonant optical field of a 150 m long optical cavity. The infrastructure constitutes a new method for geophysics, for the characterization of spatial and temporal variations of the local gravity, and is a demonstrator for future decihertz gravitational wave observation. Such an infrastructure requires ultra-high vacuum (10^{-9} mbar) on a size (150 m) and scale (36 m^3) not typically seen in underground laboratories other than CERN [2], and especially in underground environments with high humidity (up to 100%) and significant dust contamination (milimetric to micrometric porous rock particles). Here, we detail the status of the MIGA infrastructure and describe the ongoing generation and analysis of the vacuum works - this comes from tests of the prototype vacuum vessel, focusing on heating cycles, residual gas and heating analysis.

1 Introduction

MIGA, the matter-wave interferometric gravitational antenna, consists of optical [3] and atomic systems[4] that must be contained within an infrastructure sized vacuum chamber encompassing 36 cubic meters, with a working background pressure of $\sim 10^{-9}$ mbar. Creating and maintaining this vacuum is essential for atom interferometry and cold atom preparation, which require ultra-high vacuum (UHV, $\leq 10^{-8}$ mbar) to operate without significant loss to background collisions. Clean and relatively dry conditions to assemble the vacuum vessel are not available in the case of MIGA - assembly and installation takes place at the Laboratoire Souterrain à Bas Bruit (LSBB), a laboratory with high humidity and free dust particulates. Here, we demonstrate our ability to generate our required vacuum under controlled laboratory

*e-mail: benjamin.canuel@institutoptique.fr

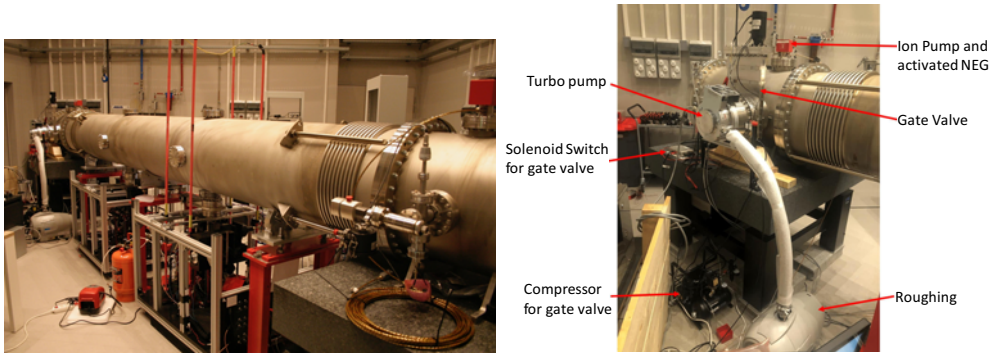

Figure 1. Standard Tube Prototype at LP2N undergoing vacuum generation and the pumping group. The diameter, steel quality, testing regime from the manufacturer, and production line are all the same for the MIGA infrastructure tubes, making this an accurate testbed for our demonstration. The two end chambers contain optics and there is space beneath the tube for two atomic sources. The pump group is connected to an end cap through a CF200 gate valve. A compressor feeds the gate valve circuit to keep the gate closed.

conditions. We show the required laboratory vacuum tests on a prototype MIGA vacuum vessel including pump down tests, baking, as well as power dissipation estimations and residual gas analysis (RGA). We examine how we achieve vacuum, maintain it, and monitor it as well as detail a system for back-filling the vacuum chamber. Based on our result, we can expect operating pressures in the region of 10^{-9} mbar for MIGA.

2 Pumping Equipment

We perform our tests on a short prototype section of tube, the LP2N gradiometer, see Fig. 1. It is composed of three tubes, the primary being 6.35 m in length, with an inner radius of 0.25 m, and wall thickness of 5 mm. The other two chambers are special end caps where there is room for an in-vacuum breadboard for optics as well as various connections for vacuum accoutrements - these are of length 0.8 m, with all other details being the same as the primary, see Fig. 2. With the addition of two atomic sources [4], the total volume comes to ~ 1.6 m^3, one order of magnitude below MIGA but four above typical cold atom systems which are typically of a volume $\sim 10^{-3}$ m^3. Maintained at UHV, MIGA is different in only one regard, in that it is five orders of magnitude larger in volume. This requires a scaling of the size of primary pumping group and secondary pumps that provide vacuum maintenance - we utilize the same pumps for this prototype that are used for MIGA [5].

We consider two types of pumps - gas transfer or gas adsorption/capture; we employ both. We employ turbo-molecular pumps (Agilent Turbo-V 1001 Navigator, 900 l/s H_2, compression ratio 10^{-6} with backing pump Agilent IDP-15 Dry Scroll, 4.3 l/s) and combination ion/non-evaporable getter (NEG) pumps (SAES D100-5 and D2000-5, NEG alloy ST 172 with 100 l/s and 2000 l/s H_2, standard diode type ion element 15[6] l/s and 32[15] l/s CH_4[Ar]), respectively. We use a residual gas analyzer (SRS RGA100) to monitor partial pressures coupled with two types of total pressure gauges - inverted magnetron (Agilent IMG-300) for UHV and capacitance (Agilent ConvecTorr, thermocouple gauge) for low vacuum (LV). Our pressure measurement range covers atmosphere to 10^{-4} mbar (LV) and 10^{-3} to 10^{-11} mbar (UHV). Our system is entirely typical for generating UHV in a cold atom experiment, but the size and pumping speed of the groups are distinct.

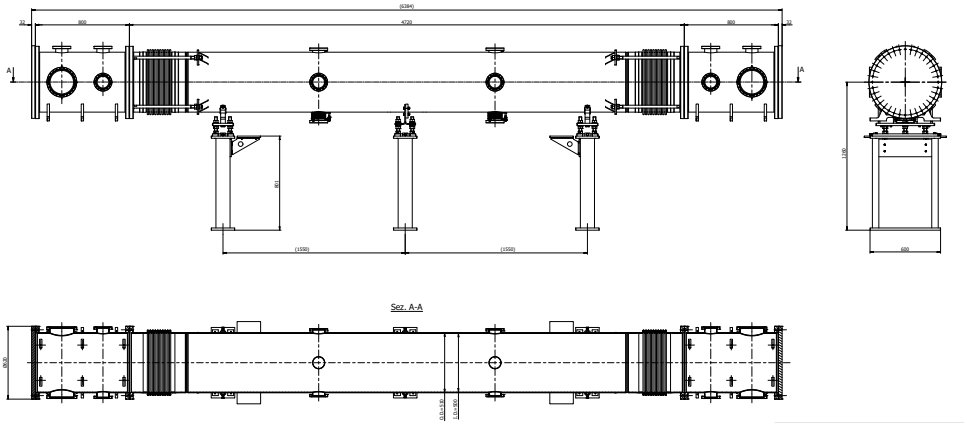

Figure 2. Scale diagram of the prototype system. The end caps are unique to the prototype, but all other components are directly related to the design of the MIGA infrastructure.

In our test setup, we place a set of gauges at each end cap - one next to the turbo-molecular pumping group, the other near to the dedicated RGA. The pumping group is connected to the vacuum chamber through a large gate valve (Pfeiffer/NorCal GVMP-S11542) for maximum conductance. A dry scroll pump is connected to the turbo-molecular pump by stainless steel bellows, the length of which is 1 m and of inner diameter 50 mm. The pressure regime at this point in the circuit varies between continuous flow and molecular flow, so the conductance is between 8.5 l/s and 15 l/s; the pumping speed and maximum backing pressure of the scroll pump is not strongly limited by these bellows - this pump alone is able to bring the entire system down to 10^{-3} mbar in about six hours. Within the atomic sources, the diameters of the orifices from the 2D MOT chamber to the 3D MOT chamber (2 mm) and the 3D MOT chamber to the detection chamber (19 mm) are relatively small, so these chambers experience significant differential pumping and utilize their own ion/getter pumps for vacuum maintenance, while also having separate pumping ports for roughing should they require it. They are each attached to the tube system through a gate valve.

When our turbo-molecular pump begins to spool up, the fan blades start to turn gradually from 0 to 650 Hz. During our tests, we heard and felt vibrations in the system while the pump was spooling. We performed finite element analysis, finding that the prototype vacuum chamber has a series of resonances around 200 Hz. When the turbine reaches this frequency, the entire chamber resonates - this kind of resonance significantly reduces the service life of components. We manage this resonance condition by modifying the pumping procedure: We first rough pump the system to between 10^{-2} mbar to 10^{-3} mbar and then close the gate valve, which is equivalent to blocking the direct connection between the vibration source and the chamber. We utilize the maximum spool rate to bring the turbine up to the maximum operating frequency quickly - using the soft start procedure, the slow ramp, lingers near the resonance and would eventually lead to pump damage. Once the pump passes the resonance frequency by a few hundred Hz, we open the gate valve.

3 Generating vacuum

Heating the vacuum chamber, known as baking, increases the desorption and diffusion rate of the system which in turn shortens the pumping time required to reach base pressure while

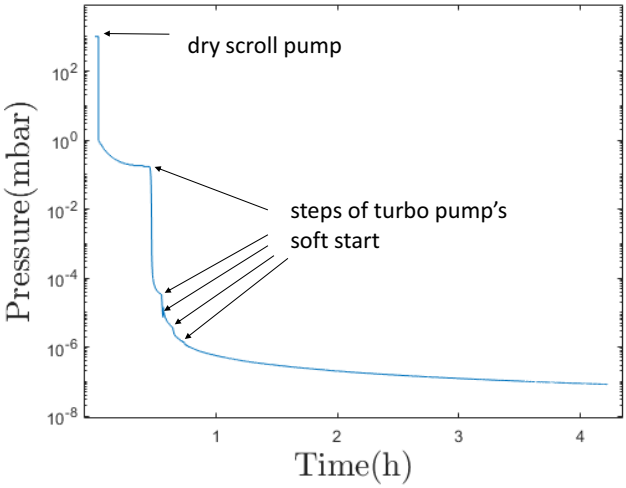

Figure 3. Pump down cycle. In this test, the dry scroll pumps the system to about 10^{-1} mbar before activation of the turbo-molecular pump. In this instance, the soft start is left for display purposes - the resonances mentioned in the text are between the second and third soft start inflections. Here, the base pressure is in the high 10^{-8} mbar region.

also reducing the base pressure. After manufacture (tested, base pressure of 10^{-8} mbar), our vacuum chamber had been baked uniformly at 250°C for 24 hours, with a reported base pressure of 1.5×10^{-11} mbar at room temperature, when pumped with a 325 l/s H_2 turbo-molecular pump (Edwards NEXT400) and a 2000 l/s H_2 NEG cartridge (SAES Capacitorr D2000, NEG alloy ST 172). The helium leak test (Hiden HALO201) showed a leak rate of $< 10^{-10}$ mbar l/s. Each tube, including the prototype, is packaged in a clean environment and sent sealed under dry nitrogen in plastic/aluminum foil bags - however, the absorption of gas and water during transportation and installation is unavoidable. The inner walls are uniformly machined to facilitate a good desorption surface, measured to be $R_a < 0.8$ μm, while the exterior walls are sand blasted to increase damage resistance, namely from water and rough handling. To obtain the required vacuum, we need to bake the system again, to evaporate water and any other contaminants attached to the inner walls - our first pumping cycle, see Fig. 3, was similar in cleanliness to after manufacture.

The power requirements and heating elements required to bake a large vacuum chamber like MIGA implies a departure from traditional small system UHV generation methodology. Of pressing importance for MIGA is to calculate the power requirements, as our access to power is limited at the facility. Generally, we require insulation material, heating elements, temperature monitoring, and temperature servo loops. For insulation, we opt for multiple thicknesses of aluminium foil, wrapped in layers; we prefer this over fiberglass for reasons of cleanliness. In the following tests, we use silicone heating bands for warming 205 liter oil drums (BRISKHEAT DHCS25) as the heating elements, repurposed for our chamber by extension of the included clasp. We found their integral temperature servo likely led to oscillations and runaway heating, due to the lack of significant thermal inertia within the chamber, given it is empty. This led to the complete destruction of the majority of band used in testing, making these unsuitable for use with MIGA. For MIGA at LSBB, we commissioned a

heating system including silicone heating bands with different, proprietary high temperature coating and glue as well as a bespoke temperature monitoring and servo system (Watlow) to circumvent these problems. We employ additional K type thermocouples, separate from the temperature servo, measured with a data logger (National Instruments 34972A LXI) for temperature monitoring.

Due to the baking cycle after manufacture and the nature of the interior surface, we found that baking the tube section at 120°C for 48 hours is sufficient to reach below the 10^{-10} mbar level, with no breadboard or optics inside the chamber. With this in mind, we sought to understand how insulation impacted the power dissipation. The three types of heat transfer are conduction, radiation, and convection - as a good conductor of heat, aluminium foil does not reduce the thermal conductivity, but critically it can effectively isolate convection when installed properly. As a result, a layer of hot air is formed around the surface of the vacuum chamber, which effectively reduces conduction and convection. The aluminum foil can also reflect the radiation of the vacuum chamber to reduce heat loss if installed with the more reflective surface towards the heating element. The reflectivity of bright aluminium foil can be as high as 88%, while that of dull embossed foil is about 80%. According to our measurements, when the inner surface of the chamber reaches 100 °C, the outermost layer of aluminium foil is only 50 °C.

We performed a test of heat capacity, see a) of Fig. 4, to understand how we could reach our target temperature with minimum power dissipated. We brought a test chamber up to 120°C and then stopped the heating. We record the temperature curve as it returns to room temperature, from which the temperature change rate $\frac{dT}{dt}$ of the vacuum chamber around 100 °C can be obtained; combined with the heat capacity of the chamber, we can calculate the heat loss rate at 100 °C. The density of the gas inside the vacuum chamber, in the molecular flow regime, is sufficiently small that the heat capacity is negligible when compared to that of stainless steel. The heat loss of the vessel per unit length (1 m) when at 100 °C is

$$q_{100\ ^\circ\mathrm{C}} = C\frac{dT}{dt},$$

where $C = cpV/L$ is the heat capacity, with our vacuum chamber material (AISI type 304 stainless steel) defined by c $\approx$ 500 J·kg^{-1}·K^{-1}, a density of $\rho \approx 8000$ kg/m^3, and a volume per unit length $V/L = 0.009$ m^2. Based on this equation and in the case of three layers of aluminum foil wrapping, the heat loss rate of the vacuum chamber per unit length near to 100 °C is 190 W. According to the temperature, a) of Fig. 4, the dissipation rate is $70W$; we estimate that the inner wall of the chamber can reach 100°C when the power dissipation of a heating element is 90 W. With this estimate, we leverage further to see that the heating power required to heat a unit length of the vacuum chamber is 244 W, and so the total estimated baking power of the 150 m vessel is about 36.6 kW to hold the interior walls of the chamber at 100°C. During a typical baking process, see b) of Fig. 4, there are some locations where the temperature does not reach 100 °C externally - this is purposeful, as some vacuum measurement equipment is limited in the baking temperature it can sustain.

4 Results

After multiple baking tests, and with internal optics and breadboard as well as the atom sources attached, we obtain a vacuum of 1.4×10^{-9} mbar, see c) of Fig. 4. After the bakes, the vacuum chamber was opened twice during the connection processes, allowing the ingress of water vapor - once for the installation of optics and again due to a leak that developed - in this respect, our result implies a better base pressure for the MIGA infrastructure. Based on

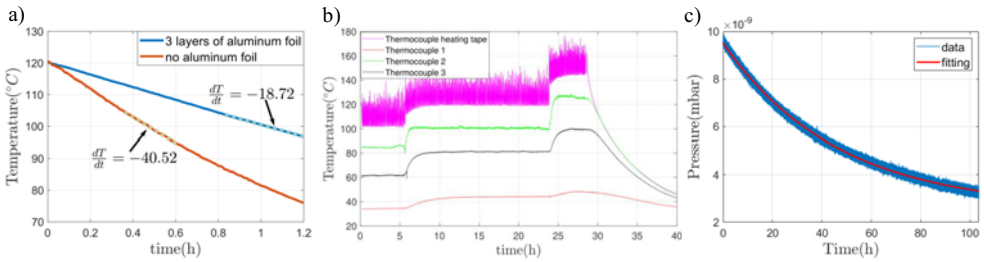

Figure 4. Heating/insulation tests and base pressure. a) Specific heat testing with and without insulation. We heating the vacuum chamber to 120 °C, stop the heating and observe the heat loss. dT/dt is in units of °C/hour. b) Typical baking test. We show a typical heating cycle and controlled raising of the temperature. Note, the thermocouple of the heating tape shows significant spikes - this led, at higher temperatures, to destruction of the heating bands. Thermocouples are positioned directly on the vacuum vessel, underneath the covering layers of foil, between bands (1), on a bellows section, and on a conflat flange without direct heating (3). c) Pumping curve of full system, reaching our present base pressure of 1.4×10^{-9} mbar.

our data, we calculate that the outgassing rate of this system in Tab. 1 - a system constructed the same way and with the same materials as the MIGA infrastructure vacuum system. No

No heating	100°C, 48 hours	100°C, 68 hours	Full System
$2. \times 10^{-11}$	8×10^{-12}	6×10^{-12}	1×10^{-11}

Table 1. Table of outgassing results. The units are in mbar $\cdot$ l $\cdot$ s^{-1}cm^{-2}. These results are comparable to the literature [6]

heating corresponds to the condition after shipping, with a heating cycle having be applied at the manufacture, and the full system includes the two atomic sources as well as internal optics and the ingress of humid air. First, we find that the an additional 20 hours past the first 48 return minimal gains in outgassing rate reduction. Second, we extrapolate based on these results - we assume that the outgassing rate is 6×10^{-12} mbar $\cdot$ l $\cdot$ s^{-1}cm^{-2} after baking. This is based on the fact that the parts of the system are baked after manufacture and cleaning for 24h at 250 C to reach a measured outgassing rate of 1×10^{-12} mbar $\cdot$ l $\cdot$ s^{-1}cm^{-2}. After shipment and installation, the system is baked at 100 C for 68 hours, carried out with a pumping speed of 920 l/s - from this we obtain and an outgassing of 6×10^{-12} mbar $\cdot$ l $\cdot$ s^{-1}cm^{-2}. Given finite pumping speed of the Antenna in Rustrel (3000 l/s), the baking step of the antenna will be longer, of the order of weeks. Nevertheless, these initial test prove that a target outgassing rate of 6×10^{-12} mbar $\cdot$ l $\cdot$ s^{-1}cm^{-2} can reasonably be reached for the final antenna with a baking at 100°C, given all parts of the system were extensively heated after manufacture. The chamber length is $L_{\mathrm{MIGA}} = 150$ m and the inner surface area is $A_{\mathrm{MIGA}} = 2\pi r\, L_{\mathrm{MIGA}} + 2\pi r^2 \approx 2.4 \times 10^6$ cm^2 so if we assuming the base pressure of the pump system is 5×10^{-11} mbar, the total pump speed required to make the pressure in the vacuum chamber reach 2×10^{-9} mbar is about 7500 l/s. For MIGA, we provide about 12500 l/s, between ion pumps, NEG cartridges, and turbo-molecular pumps, with 10000 l/s in the final stage for maintaining vacuum. For vibration noise considerations, the base pressure of the system is developed by ion pumps and NEGs, appropriately activated during at the end of the baking procedures.

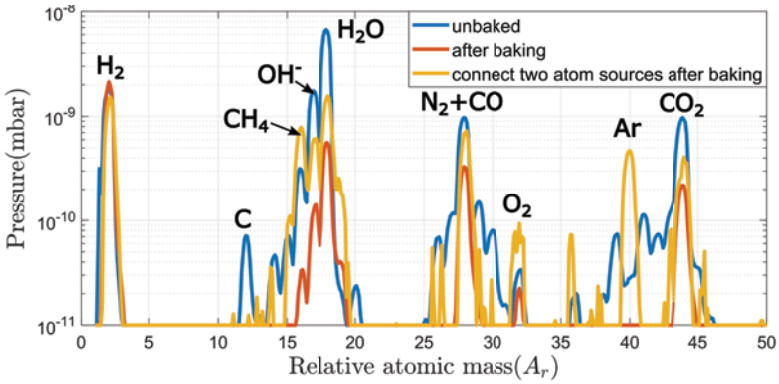

Figure 5. Residual gas analysis of the chamber. Gas molecules and clusters corresponding to each peak are labelled. The three scans correspond to the case: (blue) the vacuum chamber before baking, (red) after baking cycles, and (yellow) after baking with the two atom sources connected. The short cycle for this test led to a negligible decrease in the hydrogen partial pressure.

5 Venting

Initial construction, assembly by parts, and further improvements warrant a way to restore the vacuum chamber safely and in a controlled way back to ambient pressure, while maintaining cleanliness. We use an electronic venting valve (Pfeiffer Vacuum, EVR 116) combined with a filter (Pfeiffer Vacuum, Dust Separator SAS 16), in addition to manual safety valves and the option of a relatively clean, oil free compressor with a modest air tank. This venting valve can control the gas flow from 5×10^{-6} mbar·l/s to 1.25×10^{3} mbar·l/s, while the filter removes particles above 5 micron and absorb some water. When back filling a test chamber using the compressor, we found lower water content and did not observe any oil ingress from the pump in that we did not see an increase in any gas molecules or clusters below 100 amu on our mass spectrum analysis - the base pressure of the system remained the same. We vent the chamber in about four hours, but it can take as low as thirty minutes through one valve of this type.

6 Leak detection

We utilize the helium leak check function of the RGA to localize a leak and/or to determine the total or local leak rate[7] under UHV operation. Prior to helium leak checking, we monitor pressure changes when applying solvent to seals (acetone or IPA); if there is a leak, the solvent enters the system and evaporates. This also cools the surrounding area and creates a frozen spot of solvent that stops the leak temporarily. This creates a unique signal on pressure gauges, where the pressure spikes, and then decreases to lower than it was prior to the spike. The disadvantage of this method is that the sensitivity is limited (10^{-4}mbar), and the solvent may corrode rubber components, should there be any.

We performed leak monitoring both when connecting the optical and central chambers and when connecting the two atom sources to the vacuum chamber, see Fig. 5. We find remnants of air, water, some argon, and hydrogen from the walls of the chamber. We observe baking has an obvious and expected effect on water and air components, but our short heating cycle shown here did not significantly reduce the hydrogen partial pressure. Further, we find that connecting the atomic sources increases air and water fractions as well as argon - this

is due to a leak in a vacuum window of the atomic source that has since been found and replaced.

7 Conclusions

Here, we have presented our work on bringing a large vacuum vessel down to UHV, for application to the MIGA infrastructure at LSBB. We detail the pumping system and cycle, examine how to best utilize the available power at the facility for baking, and demonstrate UHV pressures in a prototype MIGA vacuum chamber, followed by a discussion of venting and leak detection systems. Based on our results, we can expect to reach UHV pressures on the MIGA infrastructure using the available power from the facility. Further, the preparation of the vacuum vessels in combination with our available pumping speed implies a base pressure in the 10^{-9} mbar range. Moving forward, we are constructing the MIGA infrastructure at LSBB presently, and will be utilizing the vacuum techniques detailed here to realize UHV in an underground environment.

References

[1] B. Canuel, A. Bertoldi, L. Amand, E.P. di Borgo, T. Chantrait, C. Danquigny, M.D. Álvarez, B. Fang, A. Freise, R. Geiger et al., Sci. Rep. **8**, 14064 (2018)

[2] O.S. Brüning, J. Poole, P. Collier, P. Lebrun, R. Ostojic, S. Myers, P. Proudlock, *Lhc design report* (2004), http://cds.cern.ch/record/782076

[3] D. Sabulsky, J. Junca, G. Lefèvre, X. Zou, A. Bertoldi, B. Battelier, M. Prevedelli, G. Stern, J. Santoire, Q. Beaufils et al., Scientific reports **10**, 1 (2020)

[4] Q. Beaufils, X. Zou, D.O. Sabulsky, J. Junca, A. Bertoldi, R. Geiger, B. Canuel, A. Landragin, P. Bouyer (2022), working paper or preprint, https://hal.archives-ouvertes.fr/hal-03643088

[5] B. Canuel, X. Zou, D.O. Sabulsky, J. Junca, A. Bertoldi, Q. Beaufils, R. Geiger, A. Landragin, M. Prevedelli, S. Gaffet et al., *A gravity antenna based on quantum technologies: Miga* (2022), https://arxiv.org/abs/2204.12137

[6] P. Marin, M. Dialinas, G. Lissillour, A. Marraud, A. Reboux, Vacuum **49**, 309 (1998)

[7] K. Zapfe, Tech. rep., Dt. Elektronen-Synchrotron DESY (2007)